ChemComm

FEATURE ARTICLE

Inorganic nanomaterials for bioimaging, targeted drug delivery and therapeutics

Cite this: *Chem. Commun.*, 2014, **50**, 14071

Ruizheng Liang, Min Wei,* David G. Evans and Xue Duan

Received 27th April 2014,
Accepted 10th June 2014

DOI: 10.1039/c4cc03118k

www.rsc.org/chemcomm

Inorganic nanomaterials including gold nanoparticles, mesoporous silica nanoparticles, graphene, magnetic nanoparticles, quantum dots and layered double hydroxides have become one of the most active research fields in biochemistry, biotechnology and biomedicine. Benefiting from the facile synthesis/modification, intrinsically physicochemical properties and good biocompatibility, inorganic nanomaterials have shown great potential in bioimaging, targeted drug delivery and cancer therapies. This *Feature Article* summarizes recent progress on various inorganic nanocarriers, including the background, synthesis, modification, cytotoxicity, physicochemical properties as well as their applications in biomedicine.

1. Introduction

Nanomaterials have recently become one of the most active research fields in the areas of chemistry, biotechnology, and biomedicine.[1] For biomedical applications, inorganic nanomaterials have attracted much attention in bioimaging, targeted drug delivery and cancer therapies.[2] By fabricating nanomaterials into vesicles, numerous nanocarriers have been developed for bioimaging/diagnosis and delivery of drugs and various therapeutic agents into targeted sites (Fig. 1).[3] Nanocarriers usually incorporate drugs *via* encapsulation, surface attachment or entrapping, which alters the drug pharmacokinetics *in vivo*.[4,5] Compared with pristine drugs, the nanocarrier drug delivery systems have the following advantages: (1) the efficiency of many conventional pharmaceutical therapies can be significantly improved with the aid of drug delivery systems; (2) nanocarriers show high loading capacity and sufficient protection from harsh surroundings, avoiding unnecessary drug loss; (3) nanocarriers have good solubility and stability *in vivo*, as well as a favorable route of administration and targeting, sparing normal cells and tissues; (4) nanocarriers possess high biocompatibility/biodegradability, reducing unwanted side effects.[6,7]

To date, liposomes, micelles and polymer-based nano drug delivery systems (DDSs) have reached the later stages of development, and a few have even received approval from Food and Drug Administration (FDA). However, some conventional nanocarriers suffer from the pre-leakage of drugs under harsh environmental conditions as well as uncontrollable drug release rate *in vivo*.[8,9] Recently, the development of synthesis techniques, including the ability to fabricate molecules and supramolecular structures for intended functions, has promoted the use of engineered nanomaterials. This has led to the emergence of new DDSs based on inorganic nanoparticles. Compared with the conventional DDSs, most inorganic-based DDSs are still in their pre-clinical stage of development. However, due to the ease of synthesis and modification, the inorganic nanoparticle size, shape and surface properties can be facilely controlled. In addition, integrated and multi-functional systems for bioimaging, drug delivery and therapeutics have

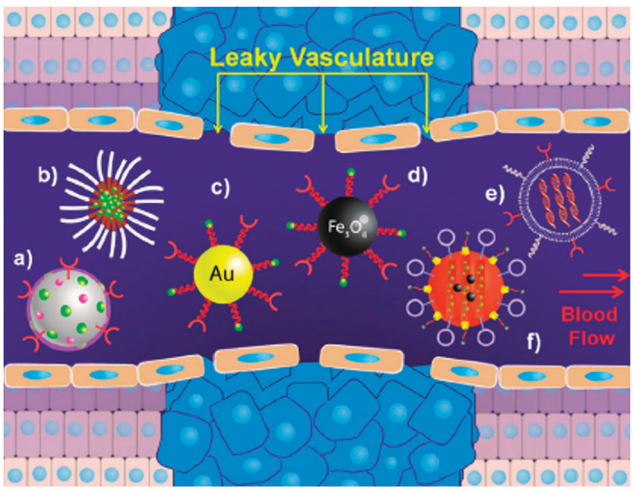

Fig. 1 Various types of nanomedicines are depicted as targeted drug delivery systems and therapeutics to a site of tumor growth in this visual representation. Conjugated targeting ligands are shown as circles or semicircles. Cargo, conjugated or housed internally, is shown as green spheres. Purple spheres represent imbedded contrast agents. A multi-functional (a) polymeric nanogel, (b) polymeric micelle, (c) gold nanoparticle, (d) iron oxide nanoparticle, (e) siRNA ensconced in a liposome delivery vector, and (f) a stimuli-responsive capped mesoporous silica nanoparticle are shown. Reproduced with permission from ref. 3.

State Key Laboratory of Chemical Resource Engineering, Beijing University of Chemical Technology, Beijing 100029, P. R. China.
E-mail: weimin@mail.buct.edu.cn; Fax: +86-10-64425385; Tel: +86-10-64412131

been achieved, by virtue of the intrinsically optical, electronic and magnetic properties of various inorganic nanomaterials. Although only a few FDA-approved inorganic nanoparticle-based nanomedicines have been used in the clinic, these novel designs and formulations are impacting conventional medicine and are showing prospective employment in diagnosis and/or treatment.[10,11]

In this *Feature Article*, we will comprehensively summarize recent progress on various inorganic nanocarriers, including the background, synthesis, modification as well as their applications in bioimaging, targeted drug delivery and therapeutics. The cytotoxicity and unique physicochemical properties of these nanocarriers for imaging or diagnosis are emphasized; multifunctional inorganic nanocarriers which combine several unique components are also reviewed. Current challenges and future strategies are discussed from the viewpoint of material design and practical application. It is anticipated that this review article will arouse more attention toward inorganic nanocarriers used in bioimaging/drug delivery systems and encourage future work to push forward the advancement of this fast-growing area.

2. Various inorganic nanocarriers used in bioimaging and drug delivery

2.1 Colloidal gold nanoparticles

Colloidal gold nanoparticles (GNPs) are good candidates as nanocarriers for biomedicine and drug delivery.[12] The importance of colloidal gold was realized when the preparation of monodispersed GNPs by the citrate reduction method was introduced. With the advantage of easy synthesis, large surface area and flexible surface chemistry, GNPs have become promising DDSs for the intracellular and *in vivo* delivery of genes, drugs and contrast agents. Moreover, by using smart polymers, it is possible to create DDSs which release their payload in response to outside stimulus.[13,14] Furthermore, owing to the high molar absorption coefficient of GNPs in the visible to near-IR region, they can be used as photothermal agents in cancer photothermal therapy. In addition, surface plasmon resonance (SPR) of GNPs is extensively studied in various biological applications ranging from bimolecular sensing to therapeutic interventions.[15]

Up to now, the most popular synthetic method for GNPs has been the Schiffrin–Brust biphasic approach developed in 1994 due to the simple steps and reagents involved.[16] Subsequently, El-Sayed *et al.*[17] and Murphy *et al.*[18] prepared GNPs with different size and shape (*e.g.*, nanorods, nanocages, nanocubes) with satisfactory reproducibility using the seed mediated growth method. Since the as-synthesized GNPs have limited types of surface capping ligands and functional groups, ligand exchange reactions and chemical modifications are necessary for employing these materials in various nanotechnology and biology applications. Murray and coworkers[19] introduced various ligand exchange reactions on alkane thiol protected GNPs, which have been further extended to the preparation of water-dispersive GNPs with terminal functional moieties. It is also possible to create gold nanostructures with active targeting capabilities *via* careful surface modification.[20,21] The active targeting takes advantage of the fact that rapidly growing cancer cells over-express certain receptors on their surface. As for the cytotoxicity of GNPs, their cellular toxicity has indeed been examined by several research groups.[22a,b] It is essential to distinguish between the toxicity of the GNP core and the exterior ligands. Generally, cationic GNPs are moderately toxic, while the same alkylthiolate-GNPs containing carboxylate termini are quite non-toxic. As further evidence of the key role of GNP ligands, large GNPs conjugated with biotin, cysteine, citrate, and glucose did not appear to be toxic in human leukemia (K562) cells at a concentration up to 250 mM in contrast to $HAuCl_4$ solutions which were found to be 90% toxic.[22c]

Most work on drug delivery of GNPs is concerned with cancer treatment.[23] Through both passive and active targeting, the concentration of drug can be increased at the tumor site while limiting the exposure of healthy tissue.[24] Furthermore, conjugation of cyclodextrins, polyethylene glycol (PEG), or polyetherimide (PEI) to the gold-cargo assemblies improves the biodistribution and suppresses toxicity. GNPs are also utilized for the intracellular or *in vivo* delivery of contrast agents, photosensitizers, antibacterial drugs and anticancer drugs. For example, El-Sayed *et al.*[25] presented a plasmonic-tunable Raman/fluorescence imaging spectroscopy strategy to study the release of doxorubicin (DOX) drug molecules from gold nanoparticles in single living cells. When DOX is bound to the surface of GNPs, the surface-enhanced Raman spectrum is sensitive but its fluorescence is quenched. When DOX is released, the Raman enhancement of GNPs is greatly reduced due to the acidic property of lysosomes, allowing for the visualization of its fluorescence signal. The Raman/fluorescence signals can be selectively switched ''ON'' and ''OFF'', achieving the DOX delivery and release process from GNPs in a real-time manner at a single living cell level.

Photothermal responses of GNPs are extensively exploited in cancer therapy. This technique was originally developed using NIR dyes, but gold nanostructures show a molar absorption coefficient 4–5 orders of magnitude stronger and exhibit higher selectivity *via* both passive and active targeting, making them ideal candidates for photothermal therapy.[26,27] The conjugation of ligands or antibodies on the surface of GNPs (*e.g.*, epidermal growth factor (EGF), folic acid (FA), anti-EGFR antibody, anti-HER2 antibody) enables cancer cell-specific labeling *in vitro* and *in vivo*. Upon irradiation, the GNPs in the labeled cells/tissues generate local heating which results in cell death *via* impairment of biomolecules and the cell membrane.[28] Therapeutic efficiency of GNPs can be improved by the combination of photothermal therapy with photodynamic therapy (PDT) and/or chemotherapy. Fei and Burda[29] developed a drug vector for PDT drug delivery by synthesizing PEG-modified GNP conjugates, which served as a water-soluble and biocompatible ''cage'' that allows the delivery of a hydrophobic drug to its site of PDT action. The dynamics of drug release *in vitro* in a two-phase solution system and *in vivo* in cancer-bearing mice demonstrates a highly efficient drug

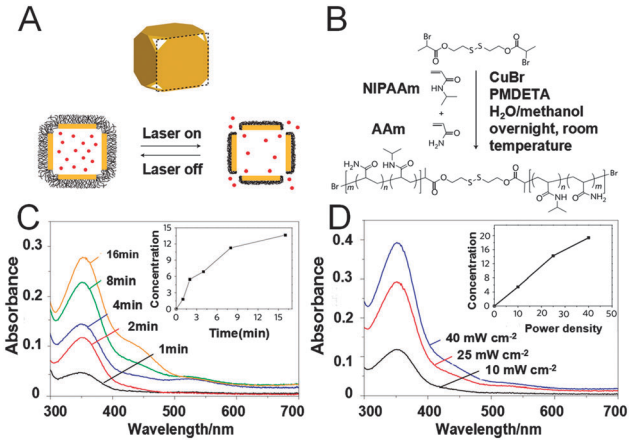

Fig. 2 (A) Schematic illustrating the release mechanism for gold nanocages coated with smart polymer chains. (B) Atom transfer radical polymerization of NIPAAm and AAm monomers as initiated by a disulfide initiator and in the presence of a Cu(I) catalyst. (C–D) Controlled release from the gold nanocages covered by a smart polymer with an LCST at 39 °C (pNIPAAm-*co*-pAAm). Reproduced with permission from ref. 13.

delivery process, in which passive targeting prefers the tumor site. With the assistance of GNP-based conjugates, the drug delivery time required for PDT was greatly reduced to less than 2 h, in comparison with 2 days for the free drug.

In addition, the photothermal effect of gold nanorods and nanocubes is a promising property for the disruption of endosomes and lysosomes and the intracellular release of trapped cargos (*e.g.*, DOX, siRNA, fluorescent dyes, and photosensitizers). Fig. 2A shows a schematic of a drug delivery system that combines the photothermal property of gold nanocages with thermo-sensitive polymers.[13] The strong binding between gold and thiol groups makes it straightforward to attach poly(*N*-isopropylacrylamide) (pNIPAAm) to the surface of the gold nanocages by using a disulfide initiator (Fig. 2B). When the gold nanocages are irradiated with a laser, the temperature rises and reaches a certain threshold at which the pNIPAAm coating undergoes a conformational change. After the collapse of the polymer, the nanocage pores are exposed, allowing for effectors pre-loaded in the interior to be released. Fig. 2C and D shows the release profiles of a PEG-conjugated alizarin dye as a function of laser irradiation time and laser power, respectively. By adjusting these parameters, a controllable release of the loaded effectors can be achieved both in solution and *in vitro*. This system is versatile, and has also been demonstrated to release both chemotherapeutic drugs and enzymes, which retained ~80% of their bioactivity after the release process.

2.2 Mesoporous silica nanoparticles

Colloidal mesoporous silica nanoparticles (MSNPs) are another important group of inorganic delivery systems. They are ideal candidates for bio-applications due to their controllable morphologies, mesostructures with biocompatibility and ease of functionalization.[30,31] Firstly, abundant silanol groups on the surface of MSNPs make them hydrophilic; the easy functionalization by various groups helps to achieve controlled holding/release of cargo molecules. Secondly, the large internal surface area and pore capacity of mesoporous materials enable a high loading of cargo molecules and prevent them from escaping into water rapidly by dissolving in an aqueous environment. This guarantees the effectiveness of the delivery system and allows more drugs to reach their therapeutic target. In addition, the MSNPs take advantage of the large pore capacity to improve the delivery of various hydrophobic anticancer drugs within the bloodstream. This is of great importance because the effectiveness of such drugs may be hampered by their low solubility in water.[32]

The modification of MSNPs can be achieved on both the exterior and interior surfaces, which is beneficial to improve nano-carrier drug delivery and provide a range of functionalities.[33] One of the key characteristics that contribute to the extensive functionalization capabilities of MSNPs is their mesoporous structure with a high surface area-to-volume ratio.[32,34] Firstly, a lot of organic molecules could be introduced into the silanol groups on the exterior surface of MSNPs *via* covalent or electrostatic interactions, and then the versatile MSNP surface can support active targeting vectors to increase the specificity of drug delivery and reduce damage in normal tissues. Moreover, recent research has revealed that the interior can also be functionalized to accommodate specific cargo molecules (drugs, nucleic acids and proteins for therapeutic purpose).[32,35,36] Before MSNPs can be effectively applied in DDSs, their cellular uptake and cytotoxicity properties have to be investigated. Cellular uptake of MSNPs and their good biocompatibility were confirmed with both healthy and cancer cell lines.[37–39] Several research groups have demonstrated that cell uptake and cellular toxicity of MSNPs depend on the particle size, shape, surface charge and functional groups.[40,41] No cytotoxicity is observed up to 100 mg mL^{-1} for non-modified 100 nm MSNPs,[42–45] which is far beyond the concentration required for most therapeutic treatments.

An important factor in the design of *in vivo* drug delivery vehicles is the targeting of diseased organs or tissues. This is especially important in cancer therapies, since the targeted DDSs should use a lower drug amount to achieve the expected therapeutic effect with decreased side effects in healthy tissues. Most strategies used for cell targeting depend on chemically modifying MSNPs with targeted moieties. These moieties include small nutrient molecules such as mannose or FA, peptides, proteins and antibodies. For example, Rosenholm *et al.*[46] developed a selective nanoparticulate system for cancer cell targeting based on PEI-functionalized and FA-conjugated MSNPs. The PEI–MSNP hybrid nanoparticles are nontoxic and can be specifically endocytosed using FA as the targeting ligand. The total number of particles internalized by the folate-receptor high cancer cells was about an order of magnitude larger than that internalized by folate-receptor low normal cells, demonstrating a promising application in targeted drug delivery for cancer treatment or imaging agents for early tumor diagnosis.

In recent years, MSNPs usually serve as the scaffold for a facile loading of imaging and therapeutic agents for both

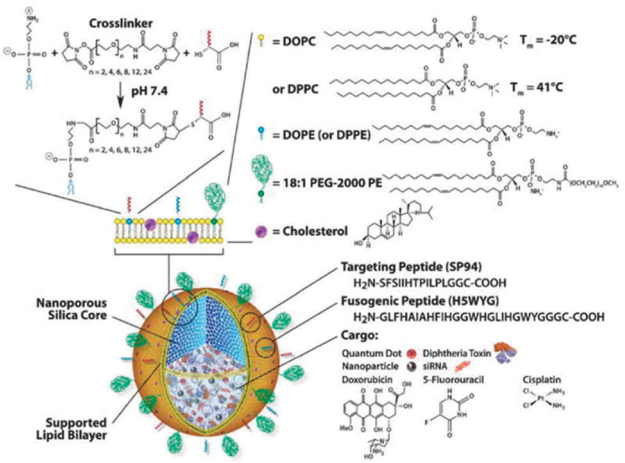

Fig. 3 Schematic illustration of the nanoporous particle-supported lipid bilayer, depicting the disparate types of therapeutic and diagnostic agents that can be loaded within the nanoporous silica core, as well as the ligands that can be displayed on the surface of the supported lipid bilayer. Reproduced with permission from ref. 48.

diagnostics and therapy.[47] Much research endeavor has been dedicated to the combination of imaging agents (quantum dots, Fe_3O_4, carbon dots, gold nanoparticles) and therapeutic drugs upon MSNP platforms. The mesoporous cavities of MSNPs can incorporate a wide variety of organic molecules (*e.g.*, drugs, proteins, nucleic acids or photosensitizers), which makes them promising candidates for theranostic applications. For example, Brinker and coworkers have developed MSNP-supported lipid bilayers as a theranostic platform (Fig. 3).[48] By synergistically combining features of both MSNPs and liposomes, they loaded a mixture of therapeutic (drugs, siRNA and toxins) and diagnostic agents (QDs) to promote cell targeting, endosomal escape and nuclear accumulation of selected cargos. The modified system with a targeting peptide that binds to human hepatocellular carcinoma exhibits a 10^5-fold greater affinity for human hepatocellular carcinoma than for hepatocytes, endothelial cells or immune cells. Furthermore, the capacity of the high-surface-area nanoporous core combined with the enhanced targeting efficacy enables the fluid supported lipid bilayer to kill a drug-resistant human hepatocellular carcinoma cell, representing a 10^6-fold improvement over comparable liposomes.

2.3 Graphene

Graphene, which is an atom thick monolayer of carbon atoms arranged in a two-dimensional honeycomb structure,[49] has been extensively explored for applications in a large variety of fields including quantum physics, nanoelectronic devices, transparent conductors, energy research and catalysis.[50–54] In recent years, graphene, graphene oxide (GO) and reduced graphene oxide (RGO) have also attracted significant interest in the field of biomedicine.[55–58] Due to the excellent physicochemical and mechanical properties, single-layered graphene has been widely explored as a novel nano-carrier for drug and gene delivery. For the intrinsic near-infrared (NIR) optical absorption, graphene-based photothermal therapy has been explored, achieving excellent anti-tumor therapeutic efficacy. Moreover, a variety of inorganic nanoparticles can be incorporated onto the surface of nano-graphene, resulting in graphene-based nanocomposites with interesting optical and magnetic properties useful for multi-modal imaging and cancer therapy. In addition, the toxicity of graphene-based materials *in vitro* and *in vivo* has been studied by many research groups.[59,60] It was found that both surface chemistry and particle size play key roles in controlling the biodistribution, excretion and toxicity of nano-graphene. Raw graphene or as-prepared GO without further functionalization appears to be toxic, while GO derivatives with biocompatible surface coatings show no significant side effects in cells in the tested dose range.[59] Nano-graphene with ultra-small size with biocompatible coatings can be cleared out from the body after systemic administration, without rendering noticeable toxicity to the treated mice at a tested dose (20 mg kg^{-1}).[61]

Many studies have been made on the fabrication of graphene and its derivatives for many different application purposes. Graphene can be produced through either bottom-up approaches (*e.g.*, the chemical vapor deposition (CVD)) and chemical methods (*e.g.*, solvothermal and organic synthesis), or top-down routes including mechanical, physical and chemical exfoliation methods.[62,63] GO is obtained by treating graphite with strong oxidizers, while RGO is often obtained *via* the graphite oxide exfoliation-chemical reduction route.[64] Although GO is soluble in water, its aggregation would occur in physiological buffers due to screening of the electrostatic charges and nonspecific binding of proteins onto its surface. Therefore, the surface modification of GO is the key to improve its biocompatibility and to control its behavior in biological systems. Depending on different application purposes, various surface coating strategies, including covalent and non-covalent approaches, have been developed to engineer functionalized graphene-based materials for use in biomedicine.[56–58] GO, rich in carboxylic acid groups, can be subsequently functionalized with a biocompatible polymer such as PEG (PEGylation). In 2008, Dai and co-workers for the first time applied six-armed PEG-amine stars to functionalize GO by conjugating amino groups on PEG to carboxyl groups on GO. The resulting PEGylated nano-GO (nGO-PEG) material with ultra-small size (5–50 nm) exhibited excellent stability in several biological solutions including serum.[65] Besides covalent chemical reactions, graphene can also be non-covalently functionalized by polymers or biomolecules *via* hydrophobic interactions, p–p stacking, or electrostatic binding to improve its stability in aqueous solutions.[61]

The intrinsic properties of graphene, such as ultrahigh surface area and large sp^2 hybridized carbon area, make graphene-based nanomaterials promising carriers for efficient drug and gene delivery. By conjugating functionalized GO or RGO with targeting ligands, selective drug delivery toward specific cancer cells has been realized. GO with different surface functionalization has been exploited as a nano-carrier for loading of a number of chemotherapy drugs including DOX,[66] camptothecin (CPT),[67] SN38 (an analog of CPT)[65] and ellagic acid,[68] by either physical adsorption or covalent conjugation. In 2008, Dai *et al.*[65] reported

that GO can be used for loading (*via* p–p stacking) and delivery of aromatic water-insoluble cancer drugs such as SN38. Intriguingly, it was found that the new delivery vehicle exhibited better efficacy than irinotecan. To enable targeted drug delivery to a specific type of cells, Dai *et al.* reported that nGO-PEG can be conjugated with an anti-CD20 antibody, rutixan, and then loaded with DOX for selective killing of B cell lymphoma.[66] FA was also chosen by several other groups as another targeting ligand for drug delivery. Controlled loading of DOX and CPT onto FA-conjugated GO was investigated by Zhang *et al.*,[69] and a linear correlation was observed between the loading ratio and the drug concentration.

One unique advantage of graphene-based cancer therapeutics is the multi-functionalities of this nano-platform, useful for combined cancer therapies.[70] For example, Chlorin e6 (Ce6) was loaded on the surface of PEGylated nano-GO *via* p–p stacking, yielding nGO-PEG–Ce6 nanocomposite drug which shows synergistic photothermal treatment plus PDT.[57] The loaded Ce6 on the nano-carrier induces a photodynamic destruction effect on cancer cells, while an extra photothermal effect of nGO-PEG under 808 nm NIR irradiation not only directly kills cells, but also increases the cell membrane permeability to further enhance the PDT efficacy (Fig. 4). In addition, the photothermal effect of nGO-PEG was also applied together with chemotherapy by Zhang *et al.* for combined cancer treatment.[71] In this work, DOX was loaded on the surface of nGO-PEG, in which photothermal therapy originating from NIR absorption of nGO-PEG and chemotherapy resulting from DOX were carried out simultaneously. Compared with individual chemotherapy or photothermal therapy, the combined chemo-photothermal therapy leads to a much higher therapeutic efficacy in terms of *in vivo* cancer treatment in a mouse model. Treating cancer by various therapeutic approaches as a combined therapy would decrease the dosage of drugs and thus may alleviate side effects during treatment.[70]

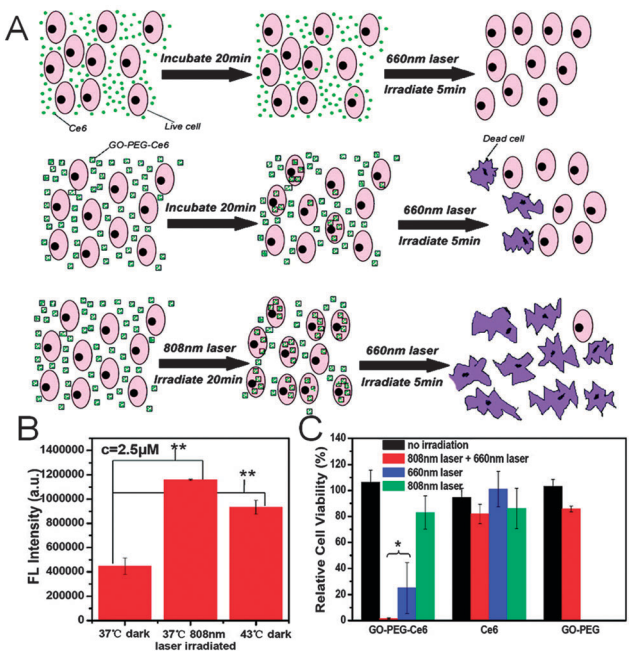

Fig. 4 Photothermally enhanced PDT. Ce6 loaded nGO-PEG (nGO-PEG–Ce6) was used in this study. (A) A scheme of photothermally enhanced PDT. (B) Cell uptake of nGO-PEG–Ce6 in different treatment groups at a Ce6 concentration of 2.5 mM. The concentration of Ce6 was determined by the measured fluorescence intensities of cell lysate samples. (C) Relative viabilities of KB cells treated with nGO-PEG–Ce6, Ce6 and nGO-PEG at a Ce6 concentration of 2.5 mM. Reproduced with permission from ref. 57.

2.4 Magnetic nanoparticles

Magnetic nanoparticles (MNPs) such as Fe_3O_4 magnetite and γ-Fe_2O_3 maghemite are particularly appealing due to their super-paramagnetic properties, tunable size and other biological functionalities.[72,73] When the particle size is smaller than the single domain limit, MNPs exhibit superparamagnetism at room temperature. Owing to these unique magnetic properties as well as their conjugation with many biological and drug molecules, MNPs have shown widespread applications in biological and medical science, for instance, in multimodal imaging, targeted drug and gene delivery, hyperthermia for cancer treatment, biomedical separation, and tissue repair.[74–77]

MNPs have traditionally been regarded as innocuous for *in vivo* applications because iron is an element present in our bodies at relatively high concentrations and MNPs can be degraded and cleared from circulation by endogenous pathways. Iron overload shows severe toxicity in humans only at a high concentration (above 60 mg Fe per kg), far beyond the concentration below 1 mg Fe per kg used in contrast agents like Endorem, although some reports have shown significant influence of the coating on the final cytotoxicity.[78,79] Moreover, the hydrodynamic size and charge of a nanoparticle are two factors that seem to be closely related to its potential toxic effects. A number of synthetic protocols have been reported for the preparation of MNPs (*e.g.*, microemulsion methods, solvothermal–hydrothermal protocols, electrochemical approaches, laser pyrolysis, *etc.*).[80–82] Regarding the biomedical applications, two preparation techniques account for more than 95% of the reports: co-precipitation of iron salts and thermal decomposition of organometallic compounds.

The first step for the preparation of targeted/therapeutic MNPs is the modification of an organic shell surrounding the magnetic core. This reaction would yield a water-soluble biocompatible product with chemically reactive groups available for further functionalization. One way is ligand exchange, in which the organic molecules capping the nanoparticle core are stripped off and substituted with more suitable ones; another promising option involves the use of molecules with terminal carboxylic groups.[83] The next step is the modification of nanoparticle surface with targeted molecules able to deliver to the desired site and/or with drugs for cancer treatment. A number of natural or synthetic materials have been used as model targeting moieties. Examples are FA (directed against folate receptor, CD71), RGD peptides (directed against $\alpha_v\beta_3$ integrin), and trastuzumab (antibody against HER2 receptor).

Magnetic resonance imaging (MRI), which is based on computer-assisted imaging of relaxation signals of proton spins

within the human internal organs excited by radiofrequency waves under a gradient magnetic field, has become a useful diagnostic tool in medical science.[84] Although MRI currently available can provide adequate images, it suffers from low sensitivity as well as insufficient spatial or temporal resolution. Therefore, many attempts have been made to combine two or more imaging modalities while eliminating or reducing their disadvantages. These include the assessment of MRI/optical properties by MRI/PET, MRI/CT and triple-modality imaging. The combination of MRI and CT imaging is highly desirable to realize high resolution, high sensitivity and excellent soft-tissue contrast. For example, Lee and Cho[85] synthesized biocompatible Fe_3O_4–TaO_x core–shell NPs, which can provide complementary information from CT and MRI (Fig. 5). Newly formed blood vessels in the tumors can be clearly imaged by CT, and the tumor microenvironment, including the hypoxic and oxygenated regions, can be evaluated using MRI. In addition, to bridge the gaps in resolution and sensitivity, development of specific contrast agents for both optical and MR imaging is highly desirable. Labhasetwar *et al.*[86] developed MNPs with optical imaging properties using NIR dyes to quantitatively determine their long-term biodistribution and tumor localization with and without an external magnetic field in mice with xenograft breast tumors. With the use of highly sensitive optical imaging, it may be possible to evaluate how formulation characteristics increase the accumulation of MNPs in tumors. Moreover, MRI/PET bimodal imaging has great potential in clinical oncology due to its improved soft-tissue contrast and superior spatial registration. Matsuda *et al.*[87] illustrate the impact of voxel-based MRI-guided PVE correction in functional FDG-PET brain imaging. A high sensitivity and excellent soft-tissue contrast would be desired by the MRI/PET bimodal imaging. The implementation of a new block detector in a fully simultaneous MRI/PET scanner will certainly open new possibilities in preclinical and clinical studies, diagnosis and therapy. On the heels of the rapid development of biomedical imaging, triple-modality imaging probes in optical imaging/PET/MRI have also attracted research interest.[88]

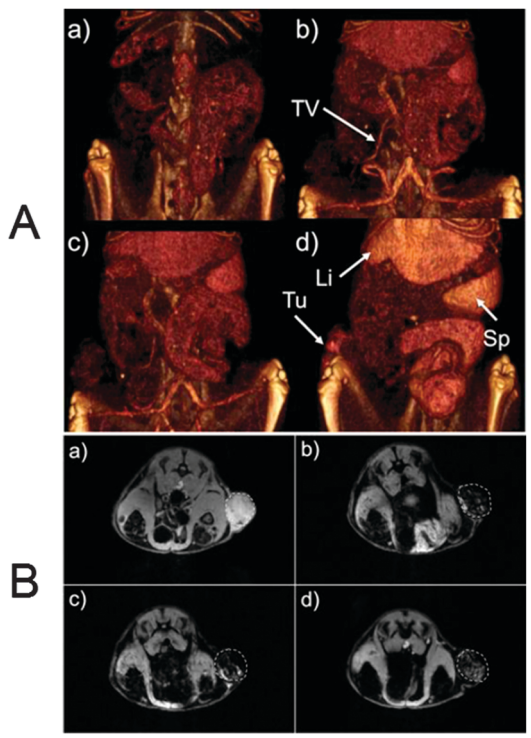

Fig. 5 (A) *In vivo* X-ray CT images of a rat (a) before and (b) 1 h, (c) 2 h, and (d) 24 h after the injection of Fe_3O_4–TaO_x core–shell NPs (840 mg kg^{-1}). TV, Li, Tu, and Sp indicate the tumor-associated vessel, liver, tumor, and spleen, respectively. (B) *In vivo* T_2-weighted MRI images of a rat bearing a MAT III B tumor (a) before and (b) 1 h, (c) 2 h, and (d) 24 h after the injection of Fe_3O_4–TaO_x core–shell NPs (840 mg kg^{-1}). Reproduced with permission from ref. 85.

Magnetic thermotherapy using MNPs is a new technique for interstitial hyperthermia and thermoablation based on magnetic field-induced excitation of biocompatible superparamagnetic nanoparticles.[89,90] When the local tumor region is exposed to an external alternating magnetic field and the temperature increases to 42–43 °C, necrotic death would occur in cancer cells without damaging the surrounding normal tissue. To date, a number of MNPs with different functionalized surface have been designed for thermotherapy of tumors. Jordan *et al.* exploited aminosilane- and dextran-coated superparamagnetic iron oxide nanoparticles (SPIONs), respectively, for thermotherapy in a rat tumor model.[91] The effectiveness of treatment was determined by the survival time of animals and histopathological examinations of the brain and tumor. Thermotherapy with aminosilane-coated nanoparticles showed a 4.5-fold prolongation of survival, while the dextran-coated particles did not indicate any advantage. Fortin *et al.* investigated the anionic SPIONs with uniform size, magnetic anisotropy and carrier fluids as well as their efficiency as heat mediators.[92] The results show that the SPIONs can serve as versatile mediators for magnetic hyperthermia in various media and appear to be a good platform for the attachment of various targeting molecules. Therefore, magnetic hyperthermia combined with other therapeutic methods such as radiation or chemotherapy will provide a synergistic therapeutic effect.

2.5 Quantum dots

Quantum dots (QDs), semiconductor nanoparticles with unique photo-physical properties, have become one of the dominant classes of imaging probes as well as universal platforms for engineering of multifunctional nanodevices.[93,94] Compared with dye molecules, QDs possess the advantages of size-dependent tunable absorption and emission, one-photon/multi-photon absorption and exceptional photostability. In particular, narrow photoluminescence bands of QDs are beneficial for minimizing bleeding during multiplexed imaging; bright and stable photoluminescence of QDs permits durable and sensitive bio-imaging even at the single-molecule level.[93] Therefore, the superior optical properties make them powerful sources to advance device technology and biotechnology.

Generally, highly fluorescent QDs can be prepared by using organometallic routes and ligand exchange reactions, and surface modifications are necessary for biological applications.

Capping QD surface with thiols is a versatile approach for both exchanging hydrophobic QDs from organic to aqueous phase and introducing functional groups for bioconjugation. Coating or conjugation of polymers onto QD surface is another method for achieving enhanced biocompatibility and extending stability against hydrolysis and biochemical reactions. Gao *et al.*[95] successfully over-coated CdSe/ZnS QDs with a tri-block amphiphilic copolymer, which protects QDs against hydrolysis and enzymatic degradation. In addition, several researchers have shown that encapsulation of QDs in silica shells significantly improves their stability and compatibility in aqueous phase. For instance, Correa-Duarte *et al.*[96] firstly conjugated a layer of 3-mercaptopropyl trimethoxysilane (MPS) on the surface of citrate-stabilized CdS QDs, followed by coating of a silica layer from sodium silicate.

Recently, bioconjugated QDs have become regular parts of biology for sensing, gene and drug delivery, and cellular and biomolecular imaging.[97] Labeling of cells by using bioconjugated QDs can be classified into nonspecific and targeted formulation. Covalent or non-covalent conjugates of QDs with antibodies, proteins, peptides, aptamers, nucleic acids and liposomes are regarded as bioconjugated QDs, which have been extensively used for direct and indirect labeling of extracellular proteins and subcellular organelles. For example, Bentzen *et al.*[98] found that CdSe/ZnS QDs coated with amphiphilic poly(acrylic acid) (AMP) nonspecifically bind to human epithelial kidney (HEK) cells to a greater extent than to mouse fibroblast cells (NIH3T3). Derfus *et al.*[99] depicted the nuclear localization signal (NLS)-conjugated QDs in comparison with the cytoplasmic location of rhodamine dextran (Fig. 6A). Similarly, mitochondrial localization signal (MLS)-conjugated QDs was observed around mitochondria by co-localization of QDs and MitoTracker Red (Fig. 6B). Therefore, the specific labeling of cellular tissue by the targeted conjugates of QDs would immensely promote their applications in biomedicine and diagnosis.

Although cell imaging and labeling are the main biological applications of QDs, multimodal imaging probes based on QDs and other contrast agents for *in vivo* applications would result in higher resolution and sensitivity. Pellegrino[100] prepared trifunctional polymer nanobeads by using a mixture of magnetic nanoparticles, quantum dots, and an amphiphilic polymer, followed by functionalization of the bead surface with folic acid. The employment of an external magnetic field to the magnetic-fluorescent nanobeads enables the quantitative accumulation of the beads within a few hours. Furthermore, it achieved specific targeting of cancer cells due to the over-expressing FA immobilized on the surface of nanobeads. Fan and Ding[101] reported capping QDs onto magnetite nanorings with a high luminescence and magnetic vortex core, which successfully served as a new magnetic fluorescent nanoprobe. The obtained multicolor QD capped magnetite nanorings exhibit a much stronger magnetic resonance (MR) T_2* effect where the r_2* relaxivity and r_2*/r_1 ratio are 4 times and 110 times larger than those of a commercial superparamagnetic iron oxide. The multiphoton fluorescence imaging and cell uptake of this magnetic fluorescent nanoprobe were also studied by using MGH bladder cancer cells, and the exploratory experiments showed that it can be used as a promising dual-modality nanoprobe for intracellular imaging and therapeutic application. Nevertheless, the cytotoxicity of cadmium-based QDs resulting from the accumulation of QDs within the body and the release of toxic Cd^{2+} ions, continues to be a major challenge in the advancement of *in vivo* imaging. Therefore, how to prevent *in vivo* QD accumulation and degradation has become a priority to assess the clinical and bio-nanotechnology prospective of QDs.

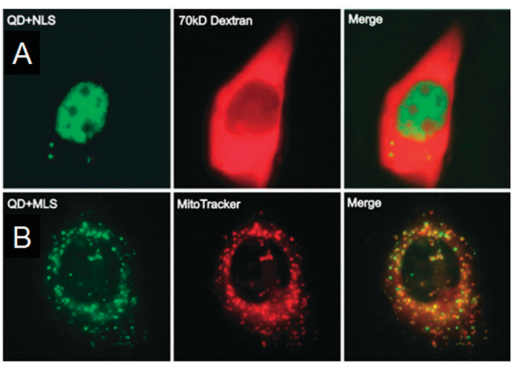

Fig. 6 Photoluminescence images of HeLa cells (A) co-microinjected with QD–NLS and 70 kDa rhodamine dextran, and (B) microinjected with QD–MLS conjugates followed by colocalization with MitoTracker Red. Reproduced with permission from ref. 99.

2.6 Layered double hydroxides

Layered double hydroxides (LDHs) are a class of naturally occurring and synthetic materials generally expressed by the formula $[M^{2+}_{1-x}M^{3+}_{x}(OH)_2](A^{n-})_{x/n}\cdot mH_2O$, in which M^{2+} and M^{3+} cations are located in the brucite-like layers and A^{n-} is the charge-balancing interlayer anion.[102] By virtue of the versatility in chemical composition as well as the stability and biocompatibility of LDH materials, they have been widely explored in the fields of drug/gene delivery and biological composite materials.[103,104] LDH materials show the following advantages in drug/gene delivery and biomedicine. Firstly, the superior biocompatibility and low cytotoxicity make LDHs an ideal drug nanocarrier system. Secondly, drugs, genes and some targeted materials (*e.g.*, antibodies, proteins, peptides, aptamers, nucleic acids) can be directly loaded onto LDHs by the intercalation method without any ligand exchange reaction and surface modification. Thirdly, the intercalation of guests (*e.g.*, organic dyes or photosensitizers) into the LDH interlamellar gallery can effectively depress the aggregation of guests and enhance their dispersion and stability. In addition, LDHs can impose a controlled release of the interlamellar drug/gene, which is necessary for pharmaceutical effect.

It has been reported that the cytotoxicity of LDHs is relatively low-to-negligible towards mammalian cells.[105,106] For example, no cytotoxic effect is observed up to 1 mg mL^{-1} when treated with the HL-60 cell line.[105] Nevertheless, the high concentration of LDHs will change the cell culture conditions

(*e.g.*, pH, ionic strength), which results in some possible cytotoxicity. The loading of drugs/genes into LDHs is generally achieved by the co-precipitation and ion-exchange method. Co-precipitation in the presence of drugs is the most direct and quantitative route to obtain LDH–drug conjugates, but drugs must be able to withstand post-preparative treatments (*e.g.*, hydrothermal treatment) used to improve uniformity and crystallinity of the materials obtained. Some anions, however, such as siRNA or antisense oligonucleotides, are not able to withstand these conditions and they are better incorporated by means of anion-exchange for the synthesis of LDH–drug conjugates. For instance, Tronto *et al.*[107] intercalated a variety of pharmaceutical anions, including salicylate, citrate, glutamate and aspartame, using two different synthesis methods. Kwak *et al.*[108] synthesized LDH hybrids containing myc antisense oligonucleotides, which were delivered to leukemia cells to produce growth inhibition of HL-60 cells.

One important merit of the loading of drugs by LDHs is the sustained release capability. Low-molecular-weight heparin (LMWH) with a molecular mass of 4–6 kDa is frequently used as an anticoagulant, but suffers from some pharmaceutical limitations (*e.g.*, a short half-life of 2–4 h, low efficiency of cellular delivery and lack of oral absorption).[109] By using the anion-exchange method, LMWH was intercalated into the LDH interlayer gallery, exhibiting an enhanced stability and prolonged half-life in blood plasma. Furthermore, it was found that the interalyer LMWH was released in a sustained way. Xu *et al.*[110] elucidated the pathway for cellular uptake of LDH nanoparticles, which involves clathrin-mediated endocytosis and endosomal escape. The location of LMWH–LDH nanohybrids and endosomal/lysosomal compartments labeled with FITC and LysoTracker Red, respectively, shows that LMWH–LDH does not degrade in lysosomal compartments. When the endosome becomes more acidic through H^+-pumping, the alkaline LDH material can neutralize the endosome by slight dissolution. As a result, ion concentration within the endosome/lysosome steadily increases, leading to osmotic swelling and eventual rupture of the endosome/lysosome with the consequent release of nanoparticles into the cytoplasm. Through the modified endocytic pathway, LMWH–LDH realizes the desired sustained release and higher pharmaceutical effect.

Another advantage of the loading of drugs by LDHs is that the intercalation of guests (*e.g.*, organic dyes or photosensitizers) into the LDH interlamellar gallery can effectively depress the aggregation and enhance the uniformity and stability. For instance, metallic phthalocyanines are the most commonly used photosensitizers in PDT, but they generally suffer from serious aggregation/self-association, weak hydrophilicity and low biocompatibility, which lead to unsatisfied PDT effect.[111] In our recent work,[112] a new photosensitizer was synthesized by incorporation of zinc phthalocyanines (ZnPc) into the LDH gallery, which shows extraordinarily high anticancer behavior in PDT. The host–guest and guest–guest interactions result in the high dispersion of ZnPc in a monomeric state in the interlayer region of the LDH matrix, with high singlet oxygen production efficiency. *In vitro* tests performed with HepG2 cells reveal a satisfactory PDT effectiveness of the ZnPc/LDH photosensitizer: cellular damage as high as 85.3% was achieved with a very low dosage of ZnPc (10 μg mL^{-1}) under 650 nm irradiation. *In vivo* studies (Fig. 7) demonstrate an excellent ZnPc/LDH-induced PDT performance, with an ultralow dose (0.3 mg kg^{-1}) and a low optical fluence rate (54 J cm^{-2}). Therefore, this work provides a facile approach for the design and fabrication of inorganic–organic hybrid materials with largely enhanced anticancer behavior, which can serve as promising photosensitizers in the field of PDT.

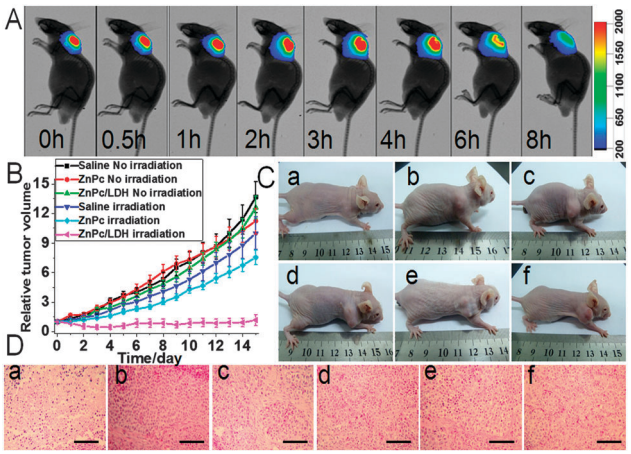

Fig. 7 (A) *In vivo* fluorescence imaging of mice after intratumoral injection with 20 μL of ZnPc(1.5%)/LDH at different time points. (B) The tumor growth curves of the six groups of mice after treatment. (C) Representative photos of mice bearing HepG2 tumors after various treatments. (D) H&E stained tumor slices collected from the six groups after 24 h of various treatments (a–f: the same as C; the scale bar is 200 μm). Reproduced with permission from ref. 112.

2.7 Multifunctional composite nanoparticles

As discussed above, various inorganic nanoparticles possess specific properties such as visible to NIR photoluminescence, photo-thermal feature or drug loading capability. Combining the above mentioned inorganic nanoparticles would result in multifunctional inorganic composites for both diagnosis and therapy of diseases. For example, MSNP-coated gold nanorods were used as light-mediated multifunctional theranostic carriers for cancer treatment.[113] The gold nanorods in the core function as both a two-photon imaging agent and a hyperthermia agent, while the outer mesoporous SiO_2 shell serves as an effective carrier with a high drug payload (Fig. 8A). The therapeutic mode of Au@SiO_2–DOX combines chemotherapy and hyperthermia, demonstrating an enhanced cancer cell killing effect through a synergistic effect. Moreover, the MSNP multifunctional platform has also been shown to encapsulate cancer drugs, superparamagnetic iron oxide nanocrystals, fluorescent tags, as well as targeting groups on the surface. This multifunctional platform achieved capabilities of drug delivery, magnetic resonance, fluorescence imaging and cell targeting simultaneously.

Moon, Hyeon and coworkers synthesized monodisperse nanoparticles consisting of dye-doped iron oxide(IO)-capped

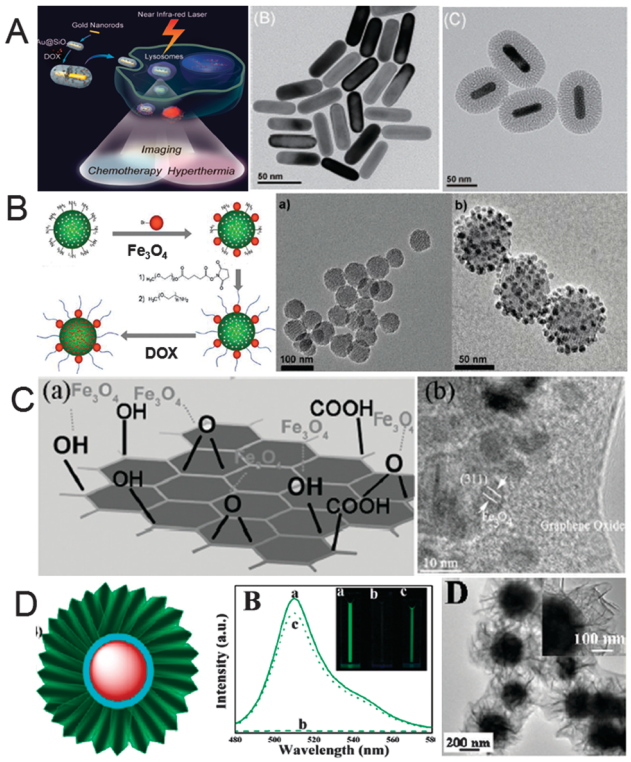

Fig. 8 (A) MSNP-coated gold nanorods loaded with cancer drug. (B) Dye-doped IO-capped MSNPs loaded with DOX and FITC. (C) Fe_3O_4 nanoparticles are covalently attached to the graphene plane. (D) *In situ* crystallization of a NiAl–LDH nanoplatelet shell on the surface of Fe_3O_4@SiO_2@AlOOH microspheres. Reproduced with permission from ref. 113, 114, 116 and 117.

MSNPs (IO@MSNPs),[114] with the particle size below 100 nm. The fluorophore (FITC or TRITC) was doped in the channels, and the IO nanoparticles were chemically attached to the exterior surface of MSNPs. The multimodal imaging capabilities of this material were tested *in vitro*; fluorescence and T_2-weighted MR images demonstrated that IO-MSNPs can be used as a multimodal probe. DOX was further loaded and the therapeutic efficacy of this system was studied by using the B16-F10 melanoma cell line. *In vivo* evaluations were carried out by intravenous injection into nude mice bearing tumors and the T_2-weighted MR signal verified passive targeting of IO-MSNPs by the enhanced permeability and retention (EPR) effect. By virtue of the facile procedure, the EPR effect and the dual-imaging capability, this composite material has great potential in simultaneous imaging and drug delivery systems (Fig. 8B). As another typical example, by growing iron oxide nanoparticles (IONP) on the surface of GO, researchers have successfully fabricated superparamagnetic GO–IONP nanocomposites which could be employed as both anticancer drug carriers and contrast agents in MR imaging.[115] Ajayan and co-workers also reported that IONP was covalently attached to the graphene plane to form GO–IONP suspensions for multimodal fluorescence and MR imaging of cells (Fig. 8C).[116]

Recently, our group[117] reported three-component microspheres containing a SiO_2-coated Fe_3O_4 magnetite core and an LDH nanoplatelet shell *via* an *in situ* growth method (Fig. 8D). The resulting Fe_3O_4@SiO_2@NiAl–LDH microspheres display three-dimensional core–shell architecture with flowerlike morphology, a large surface area and uniform mesochannels. The Ni^{2+} cations in the NiAl–LDH shell provide docking sites for histidine and the materials exhibit excellent performance in the separation of histidine (His)-tagged green fluorescent protein, with a binding capacity as high as 239 μg mg^{-1}. The microspheres show highly selective adsorption of the His-tagged protein from *Escherichia coli* lysate, demonstrating their practical applicability. Moreover, the Fe_3O_4@SiO_2@NiAl–LDH microspheres possess superparamagnetism and high saturation magnetization, which allows them to be easily separated from solution by means of an external magnetic field. The high stability and selectivity of the multifunctional microspheres toward the His-tagged protein were retained over several recycles, indicating favorable applications in protein separation.

3. Discussion and conclusion

This *Feature Article* summarizes the advancement of inorganic nanoparticles in bioimaging, targeted drug delivery and therapeutics. Inorganic nanoparticles such as GNPs, MSNPs, MNPs, QDs, LDHs and graphene have been extensively explored as nanocarriers for various biological applications ranging from bioimaging to diagnosis and therapy. The large surface to volume ratio is the common property among these nanomaterials, which is a key factor for the conjugation of various targeting molecules, contrast agents, drugs and genes at a high local concentration. Furthermore, for *in vivo* imaging and therapy applications, an important feature lies in multifunctional nanoplatforms that combine both multimodal imaging and therapeutic components. The composites of these inorganic nanomaterials show certain properties that are valuable in multiplexed bioimaging, delivery and therapeutics. For example, graphene, GNPs and QDs display visible to NIR photoluminescence; graphene, GNPs and MNPs possess satisfactory phototherapy ability; and LDHs and MSNPs exhibit high drug loading capability. In addition, through chemical and bioconjugation reactions, many functional units including targeting molecules, drugs, genes and contrast agents are combined in the formulation of imaging probes, DDSs and nanomedicines.

The ultimate goal in this field is to develop nanomaterials that allow for efficient, specific *in vivo* delivery of therapeutic agents without systemic toxicity, and the dose delivered as well as the therapeutic efficacy can be accurately monitored non-invasively over time. The emerging nanotechnology helps to build nano DDSs as a potential approach to overcome some of the barriers for efficient targeting and therapy in cancer cells. However, great efforts and innovations are needed in order to reach clinical implementation. Firstly, inorganic nanocarriers inevitably face some challenges such as premature cargo leakage, unwanted reticuloendothelial system (RES) organ capture, biodistribution, and cytotoxicity. A comprehensive resolution should be considered, including sophisticated material design,

ingenious fabrication and integrated evaluation process. Secondly, since most inorganic DDSs still remain in the preclinical stage or at the cellular and intact animal level, successful demonstrations of their biocompatibility and safety profile in clinical trials are absolutely needed. To achieve such an arduous goal, tight and deep collaborations from chemists, biologists and physicians are extremely encouraging and prospective. We firmly believe that the rapid development of both nanotechnology and biotechnology will help overcome the obstacles and push forward the progress of inorganic nanocarriers used in clinical imaging, drug delivery and therapeutics.

Acknowledgements

This work was supported by the 973 Program (Grant No. 2014CB932102), the National Natural Science Foundation of China (NSFC), the Scientific Fund from Beijing Municipal Commission of Education (20111001002) and the Fundamental Research Funds for the Central Universities (ZD 1303). M. Wei particularly appreciates the financial aid from the China National Funds for Distinguished Young Scientists of the NSFC.

Notes and references

1 V. Biju, *Chem. Soc. Rev.*, 2014, **43**, 744.
2 L. Zhang, Y. Li and J. C. Yu, *J. Mater. Chem. B*, 2014, **2**, 452.
3 L. Dykman and N. Khlebtsov, *Chem. Soc. Rev.*, 2012, **41**, 2256.
4 K. K. Cotí, M. E. Belowich, M. Liong, M. W. Ambrogio, Y. A. Lau, H. A. Khatib, J. I. Zink, N. M. Khashab and J. F. Stoddart, *Nanoscale*, 2009, **1**, 16.
5 Y.-L. Luo, Y.-S. Shiao and Y.-F. Huang, *ACS Nano*, 2011, **5**, 7796.
6 W. X. Mai and H. Meng, *Integr. Biol.*, 2013, **5**, 19.
7 T. C. Yih and M. A. Fandi, *J. Cell. Biochem.*, 2006, **97**, 1184.
8 N. Maurer, D. B. Fenske and P. R. Cullis, *Expert Opin. Biol. Ther.*, 2001, **1**, 923.
9 Y. Barenholz, *Curr. Opin. Colloid Interface Sci.*, 2001, **6**, 66.
10 D. Peer, J. M. Karp, S. Hong, O. C. Farokhzad, R. Margalit and R. Langer, *Nat. Nanotechnol.*, 2007, **2**, 751.
11 N. Kamaly, Z. Xiao, P. M. Valencia, A. F. Radovic-Moreno and O. C. Farokhzad, *Chem. Soc. Rev.*, 2012, **41**, 2971.
12 N. Lewinski, V. Colvin and R. Drezek, *Small*, 2008, **4**, 26.
13 M. S. Yavuz, Y. Cheng, J. Chen, C. M. Cobley, Q. Zhang, M. Rycenga, J. Xie, C. Kim, K. H. Song, A. G. Schwartz, L. V. Wang and Y. Xia, *Nat. Mater.*, 2009, **8**, 935.
14 (*a*) X. An, F. Zhang, Y. Zhu and W. Shen, *Chem. Commun.*, 2010, **46**, 7202; (*b*) P. Shi, K. Qu, J. Wang, M. Li, J. Ren and X. Qu, *Chem. Commun.*, 2012, **48**, 7640; (*c*) S. R. Sershen, S. L. Westcott, N. J. Halas and J. L. West, *J. Biomed. Mater. Res.*, 2000, **51**, 293.
15 K. Saha, S. S. Agasti, C. Kim, X. Li and V. M. Rotello, *Chem. Rev.*, 2012, **112**, 2739.
16 M. Brust, M. Walker, D. Bethell, D. J. Schiffrin and R. Whyman, *J. Chem. Soc., Chem. Commun.*, 1994, 801.
17 E. C. Dreaden, A. M. Alkilany, X. Huang, C. J. Murphy and M. A. El-Sayed, *Chem. Soc. Rev.*, 2012, **41**, 2740.
18 C. J. Murphy, A. M. Gole, S. E. Hunyadi, J. W. Stone, P. N. Sisco, A. Alkilany, B. E. Kinard and P. Hankins, *Chem. Commun.*, 2008, 544.
19 A. C. Templeton, W. P. Wuelfing and R. W. Murray, *Acc. Chem. Res.*, 2001, **33**, 27.
20 D. Peer, J. M. Karp, S. Hong, O. C. Farokhzad, R. Margalit and R. Langer, *Nat. Nanotechnol.*, 2007, **2**, 751.
21 L. Au, Q. Zhang, C. M. Cobley, M. Gidding, A. G. Schwartz, J. Chen and Y. Xia, *ACS Nano*, 2010, **4**, 35.
22 (*a*) N. Lewinsky, V. Colvin and R. Drezek, *Small*, 2008, **4**, 26; (*b*) C. J. Murphy, A. M. Gole, J. W. Stone, P. N. Sisco, A. M. Alkilany, E. C. Goldsmith and S. C. Baxter, *Acc. Chem. Res.*, 2008, **41**, 1721; (*c*) E. Connor, J. Mwamuka, A. Gole, C. J. Murphy and M. Whyatt, *Small*, 2005, **21**, 325.
23 M.-C. Daniel and D. Astruc, *Chem. Rev.*, 2004, **104**, 293.
24 P. Ghosh, G. Han, M. De, C. K. Kim and V. M. Rotello, *Adv. Drug Delivery Rev.*, 2008, **60**, 1307.
25 B. Kang, M. M. Afifi, L. A. Austin and M. A. El-Sayed, *ACS Nano*, 2013, **7**, 7420.
26 J. Chen, C. Glaus, R. Laforest, Q. Zhang, M. Yang, M. Gidding, M. J. Welch and Y. Xia, *Small*, 2010, **6**, 811.
27 X. Huang, P. K. Jain, I. H. El-Sayed and M. A. El-Sayed, *Lasers Med. Sci.*, 2008, **23**, 217.
28 X. Huang, I. H. El-Sayed and M. A. El-Sayed, *Methods Mol. Biol.*, 2010, **624**, 343.
29 Y. Cheng, A. C. Samia, J. D. Meyers, I. Panagopoulos, B. Fei and C. Burda, *J. Am. Chem. Soc.*, 2008, **130**, 10643.
30 A. Popat, S. B. Hartono, F. Stahr, J. Liu, S. Z. Qiao and G. Q. Lu, *Nanoscale*, 2011, **3**, 2801.
31 (*a*) S.-H. Wu, Y. Hung and C.-Y. Mou, *Chem. Commun.*, 2011, **47**, 9972; (*b*) W. X. Mai and H. Meng, *Integr. Biol.*, 2013, **5**, 19.
32 Z. Li, J. C. Barnes, A. Bosoy, J. F. Stoddart and J. I. Zink, *Chem. Soc. Rev.*, 2012, **41**, 2590.
33 N. Kamaly, Z. Xiao, P. M. Valencia, A. F. Radovic-Moreno and O. C. Farokhzad, *Chem. Soc. Rev.*, 2012, **41**, 2971.
34 M. H. Lim and A. Stein, *Chem. Mater.*, 1999, **11**, 3285.
35 S. M. Solberg and C. C. Landry, *J. Phys. Chem. B*, 2006, **110**, 15261.
36 D. Margolese, J. A. Melero, S. C. Christiansen, B. F. Chmelka and G. D. Stucky, *Chem. Mater.*, 2000, **12**, 2448.
37 J. Lu, M. Liong, J. I. Zink and F. Tamanoi, *Small*, 2007, **3**, 1341.
38 D. R. Radu, C. Y. Lai, K. Jeftinija, E. W. Rowe, S. Jeftinija and V. S. Y. Lin, *J. Am. Chem. Soc.*, 2004, **126**, 13216.
39 S. P. Hudson, R. F. Padera, R. Langer and D. S. Kohane, *Biomaterials*, 2008, **29**, 4045.
40 J. L. Vivero-Escoto, I. I. Slowing, B. G. Trewyn and V. S. Y. Lin, *Small*, 2010, **6**, 1952.
41 S. H. Wu, Y. Hung and C. Y. Mou, *Chem. Commun.*, 2011, **47**, 9972.
42 C. R. Thomas, D. P. Ferris, J. H. Lee, E. Choi, M. H. Cho, E. S. Kim, J. F. Stoddart, J. S. Shin, J. Cheon and J. I. Zink, *J. Am. Chem. Soc.*, 2010, **132**, 10623.
43 H. Meng, M. Liong, T. Xia, Z. Li, Z. Ji, J. I. Zink and A. E. Nel, *ACS Nano*, 2010, **4**, 4539.
44 J. Lu, E. Choi, F. Tamanoi and J. I. Zink, *Small*, 2008, **4**, 421.
45 J. Lu, M. Liong, Z. Li, J. I. Zink and F. Tamanoi, *Small*, 2010, **6**, 1794.
46 J. M. Rosenholm, A. Meinander, E. Peuhu, R. Niemi, J. E. Eriksson, C. Sahlgren and M. Linden, *ACS Nano*, 2009, **3**, 197.
47 S. M. Janib, A. S. Moses and J. A. MacKay, *Adv. Drug Delivery Rev.*, 2010, **62**, 1052.
48 C. E. Ashley, E. C. Carnes, G. K. Phillips, D. Padilla, P. N. Durfee, P. A. Brown, T. N. Hanna, J. Liu, B. Phillips, M. B. Carter, N. J. Carroll, X. Jiang, D. R. Dunphy, C. L. Willman, D. N. Petsev, D. G. Evans, A. N. Parikh, B. Chackerian, W. Wharton, D. S. Peabody and C. J. Brinker, *Nat. Mater.*, 2011, **10**, 389.
49 K. S. Novoselov, A. K. Geim, S. V. Morozov, D. Jiang, Y. Zhang, S. V. Dubonos, I. V. Grigorieva and A. A. Firsov, *Science*, 2004, **306**, 666.
50 K. P. Loh, Q. Bao, G. Eda and M. Chhowalla, *Nat. Chem.*, 2010, **2**, 1015.
51 A. K. Geim and K. S. Novoselov, *Nat. Mater.*, 2007, **6**, 183.
52 H. Wang, Y. Liang, T. Mirfakhrai, Z. Chen, H. S. Casalongue and H. Dai, *Nano Res.*, 2011, **4**, 729.
53 X. Huang, X. Qi, F. Boey and H. Zhang, *Chem. Soc. Rev.*, 2012, **41**, 666.
54 S. Stankovich, D. A. Dikin, G. H. B. Dommett, K. M. Kohlhaas, E. J. Zimney, E. A. Stach, R. D. Piner, S. T. Nguyen and R. S. Ruoff, *Nature*, 2006, **442**, 282.
55 L. Z. Feng and Z. A. Liu, *Nanomedicine*, 2011, **6**, 317.
56 K. Yang, J. Wan, S. Zhang, B. Tian, Y. Zhang and Z. Liu, *Biomaterials*, 2012, **33**, 2206.
57 B. Tian, C. Wang, S. Zhang, L. Feng and Z. Liu, *ACS Nano*, 2011, **5**, 7000.
58 S. A. Zhang, K. Yang, L. Z. Feng and Z. Liu, *Carbon*, 2011, **49**, 4040.
59 K. Yang, J. M. Wan, S. A. Zhang, Y. J. Zhang, S. T. Lee and Z. Liu, *ACS Nano*, 2011, **5**, 516.
60 Y. Li, Y. Liu, Y. Fu, T. Wei, L. L. Guyader, G. Gao, R. S. Liu, Y. Z. Chang and C. Chen, *Biomaterials*, 2012, **33**, 402.

61 K. Yang, L. Feng, X. Shi and Z. Liu, *Chem. Soc. Rev.*, 2013, **42**, 530.
62 S. Park and R. S. Ruoff, *Nat. Nanotechnol.*, 2009, **4**, 217.
63 D. R. Dreyer, S. Park, C. W. Bielawski and R. S. Ruoff, *Chem. Soc. Rev.*, 2010, **39**, 228.
64 W. S. Hummers and R. E. Offeman, *J. Am. Chem. Soc.*, 1958, **80**, 1339.
65 Z. Liu, J. T. Robinson, X. M. Sun and H. J. Dai, *J. Am. Chem. Soc.*, 2008, **130**, 10876.
66 X. Sun, Z. Liu, K. Welsher, J. T. Robinson, A. Goodwin, S. Zaric and H. Dai, *Nano Res.*, 2008, **1**, 203.
67 N. G. Sahoo, H. Bao, Y. Pan, M. Pal, M. Kakran, H. K. F. Cheng, L. Li and L. P. Tan, *Chem. Commun.*, 2011, **47**, 5235.
68 M. Kakran, N. G. Sahoo, H. Bao, Y. Pan and L. Li, *Curr. Med. Chem.*, 2011, **18**, 4503.
69 L. Zhang, J. Xia, Q. Zhao, L. Liu and Z. Zhang, *Small*, 2010, **6**, 537.
70 (*a*) Y. Cho and Y. Choi, *Chem. Commun.*, 2012, **48**, 9912; (*b*) Y. Cho, H. Kima and Y. Choi, *Chem. Commun.*, 2013, **49**, 1202; (*c*) D. A. Scheinberg, C. H. Villa, F. E. Escorcia and M. R. McDevitt, *Nat. Rev. Clin. Oncol.*, 2010, **7**, 266.
71 W. Zhang, Z. Guo, D. Huang, Z. Liu, X. Guo and H. Zhong, *Biomaterials*, 2011, **32**, 8555.
72 R. Qiao, C. Yang and M. Gao, *J. Mater. Chem.*, 2009, **19**, 6274.
73 R. Hao, R. Xing, Z. Xu, Y. Hou, S. Gao and S. Sun, *Adv. Mater.*, 2010, **22**, 2729.
74 H. Yang, C. Zhang, X. Shi, H. Hu, X. Du, Y. Fang, Y. Ma, H. Wu and S. Yang, *Biomaterials*, 2010, **31**, 3667.
75 P. Cherukuri, E. S. Glazer and S. A. Curley, *Adv. Drug Delivery Rev.*, 2010, **62**, 339.
76 W. Wang, Y. Xu, D. I. C. Wang and Z. Li, *J. Am. Chem. Soc.*, 2009, **131**, 12892.
77 D. M. Huang, J. K. Hsiao, Y. C. Chen, L. Y. Chien, M. Yao, Y. K. Chen, B. S. Ko, S. C. Hsu, L. A. Tai, H. Y. Cheng, S. W. Wang, C. S. Yang and Y. C. Chen, *Biomaterials*, 2009, **30**, 3645.
78 M. Mahmoudi, S. Laurent, M. A. Shokrgozar and M. Hosseinkhani, *ACS Nano*, 2011, **5**, 7263.
79 A. Asati, S. Santra, C. Kaittanis and J. M. Perez, *ACS Nano*, 2010, **4**, 5321.
80 L. H. Reddy, J. L. Arias, J. Nicolas and P. Couvreur, *Chem. Rev.*, 2012, **112**, 5818.
81 S. Laurent, D. Forge, M. Port, A. Roch, C. Robic, L. V. Elst and R. N. Muller, *Chem. Rev.*, 2008, **108**, 2064.
82 T. D. Schladt, K. Schneider, H. Schild and W. Tremel, *Dalton Trans.*, 2011, **40**, 6315.
83 J. H. Lee, Y. M. Huh, Y. W. Jun, J. W. Seo, J. T. Jang, H. T. Song, S. Kim, E. J. Cho, H. G. Yoon, J. S. Suh and J. Cheon, *Nat. Med.*, 2007, **13**, 95.
84 H. B. Na, I. C. Song and T. Hyeon, *Adv. Mater.*, 2009, **21**, 2133.
85 N. Lee, H. R. Cho, M. H. Oh, S. H. Lee, K. Kim, B. H. Kim, K. Shin, T.-Y. Ahn, J. W. Choi, Y.-W. Kim, S. H. Choi and T. Hyeon, *J. Am. Chem. Soc.*, 2012, **134**, 10309.
86 S. P. Foy, R. L. Manthe, S. T. Foy, S. Dimitrijevic, N. Krishnamurthy and V. Labhasetwar, *ACS Nano*, 2010, **4**, 5217.
87 H. Matsuda, T. Ohnishi, T. Asada, Z. J. Li, H. Kanetaka, E. Imabayashi, F. Tanaka and S. Nakano, *J. Nucl. Med.*, 2003, **44**, 1243.
88 X. Zhu, J. Zhou, M. Chen, M. Shi, W. Feng and F. Li, *Biomaterials*, 2012, **33**, 4618.
89 R. Hergt and S. Dutz, *J. Magn. Magn. Mater.*, 2007, **311**, 187.
90 J. P. Fortin, C. Wilhelm, J. Servais, C. Menager, J. C. Bacri and F. Gazeau, *J. Am. Chem. Soc.*, 2007, **129**, 2628.
91 A. Jordan, R. Scholz, K. Maier-Hauff, F. K. van Landeghem, N. Waldoefner, U. Teichgraeber, J. Pinkernelle, H. Bruhn, F. Neumann, B. Thiesen, A. V. Deimling and R. Felix, *J. Neurooncol.*, 2006, **78**, 7.
92 J. Fortin, C. Wilhelm, J. Servais, C. Ménager, J. Bacri and F. Gazeau, *J. Am. Chem. Soc.*, 2007, **129**, 2628.
93 P. Zrazhevskiy, M. Sena and X. Gao, *Chem. Soc. Rev.*, 2010, **39**, 4326.
94 V. Biju, T. Itoh and M. Ishikawa, *Chem. Soc. Rev.*, 2010, **39**, 3031.
95 X. H. Gao, Y. Y. Cui, R. M. Levenson, L. W. K. Chung and S. M. Nie, *Nat. Biotechnol.*, 2004, **22**, 969.
96 M. A. Correa-Duarte, M. Giersig and L. M. Liz-Marzan, *Chem. Phys. Lett.*, 1998, **286**, 497.
97 X. Michalet, F. F. Pinaud, L. A. Bentolila, J. M. Tsay, S. Doose, J. J. Li, G. Sundaresan, A. M. Wu, S. S. Gambhir and S. Weiss, *Science*, 2005, **307**, 538.
98 E. L. Bentzen, I. D. Tomlinson, J. Mason, P. Gresch, M. R. Warnement, D. Wright, E. Sanders-Bush, R. Blakely and S. J. Rosenthal, *Bioconjugate Chem.*, 2005, **16**, 1488.
99 A. M. Derfus, W. C. W. Chan and S. N. Bhatia, *Adv. Mater.*, 2004, **16**, 961.
100 R. D. Corato, N. C. Bigall, A. Ragusa, D. Dorfs, A. Genovese, R. Marotta, L. Manna and T. Pellegrino, *ACS Nano*, 2011, **5**, 1109.
101 H.-M. Fan, M. Olivo, B. Shuter, J.-B. Yi, R. Bhuvaneswari, H.-R. Tan, G.-C. Xing, C.-T. Ng, L. Liu, S. S. Lucky, B.-H. Bay and J. Ding, *J. Am. Chem. Soc.*, 2010, **132**, 14803.
102 G. Hu and D. O' Hare, *J. Am. Chem. Soc.*, 2005, **127**, 17808.
103 M. Darder, P. Aranda and E. R. Hitzky, *Adv. Mater.*, 2007, **19**, 1309.
104 E. R. Hitzky, M. Darder, P. Aranda and K. Ariga, *Adv. Mater.*, 2010, **22**, 323.
105 W. M. Kriven, S.-Y. Kwak, M. A. Wallig and J.-H. Choy, *MRS Bull.*, 2004, **29**, 33.
106 Z. P. Xu, T. L. Walker, K.-L. Liu, H. M. Cooper, G. Q. Lu and P. F. Bartlett, *Int. J. Nanomed.*, 2007, **2**, 163.
107 J. Tronto, M. J. d. Reis, F. Silvério, V. R. Balbo, J. M. Marchetti and J. B. Valim, *J. Phys. Chem. Solids*, 2004, **65**, 475.
108 S.-Y. Kwak, Y.-J. Jeong, J.-S. Park and J.-H. Choy, *Solid State Ionics*, 2002, **151**, 229.
109 Z. Gu, A. C. Thomas, Z. P. Xu, J. H. Campbell and G. Q. Lu, *Chem. Mater.*, 2008, **20**, 3715.
110 Z. Gu, B. E. Rolfe, A. C. Thomas, J. H. Campbell, G. Q. Lu and Z. P. Xu, *Biomaterials*, 2011, **32**, 7234.
111 B. A. Bench, A. Beveridge, W. M. Sharman, G. J. Diebold, J. E. Lier and S. M. Gorun, *Angew. Chem., Int. Ed.*, 2002, **41**, 748.
112 R. Liang, R. Tian, L. Ma, L. Zhang, Y. Hu, J. Wang, M. Wei, D. Yan, D. G. Evans and X. Duan, *Adv. Funct. Mater.*, 2014, **14**, 3144.
113 Z. Zhang, L. Wang, J. Wang, X. Jiang, X. Li, Z. Hu, Y. Ji, X. Wu and C. Chen, *Adv. Mater.*, 2012, **24**, 1418.
114 J. E. Lee, N. Lee, H. Kim, J. Kim, S. H. Choi, J. H. Kim, T. Kim, I. C. Song, S. P. Park, W. K. Moon and T. Hyeon, *J. Am. Chem. Soc.*, 2010, **132**, 552.
115 X. Yang, Y. Wang, X. Huang, Y. Ma, Y. Huang, R. Yang, H. Duan and Y. Chen, *J. Mater. Chem.*, 2011, **21**, 3448.
116 T. N. Narayanan, B. K. Gupta, S. A. Vithayathil, R. R. Aburto, S. A. Mani, J. Taha-Tijerina, B. Xie, B. A. Kaipparettu, S. V. Torti and P. M. Ajayan, *Adv. Mater.*, 2012, **24**, 2992.
117 M. Shao, F. Ning, J. Zhao, M. Wei, D. G. Evans and X. Duan, *J. Am. Chem. Soc.*, 2012, **134**, 1071.